

Equivalent circuit model for the insulated core transformer

Bo Yang¹ · Lei Cao² · Jun Yang² · Sheng-Chi Yan¹ · Yi-Bin Tao¹

Received: 26 June 2015 / Revised: 30 July 2015 / Accepted: 8 September 2015 / Published online: 12 May 2016

© Shanghai Institute of Applied Physics, Chinese Academy of Sciences, Chinese Nuclear Society, Science Press China and Springer Science+Business Media Singapore 2016

Abstract The design of the insulated core transformer (ICT) needs to consider the flux leakage effects. An equivalent linear circuit model is proposed based on the principle of duality. It is composed by two types of leakage inductances: conventional leakage between windings and special leakage introduced mainly by the insulation gaps. The values of leakage inductances depend on the dimensions of the core, gaps, or windings and the property of magnetic materials. The circuit allows for quantitatively evaluating influences of ICT internal parameters on its output properties. The winding self- and mutual inductance matrix is mathematically converted to derive the inductance formula. As an example, the leakage parameters of a six-stage two-dimensional (2D) ICT are calculated and analyzed.

Keywords High-voltage power supply · Insulated core transformer · Leakage inductance · Equivalent circuit

1 Introduction

Industrial irradiation has become the fundamental application area of electron beam accelerators in recent years [1–4]. A high-voltage generator is the kernel

component in the power supply for accelerating electrons. The direct current (DC) voltage source based on insulated core transformer (ICT) technology has advantages over others, from several hundred kV to a few MV. It was invented by Van de Graaff to convert industrial frequency (50 Hz) alternating current (AC) voltage to high DC voltage [5]. The magnetic core of this step-up transformer is divided into several electrically insulated and magnetically coupled sections by thin insulation layers (usually teflon or mica sheets). Each section has its own secondary winding, and all the windings are arranged in a top–bottom configuration. The AC output from each winding is converted into DC voltage by a double-rectifier circuit, and all the output terminals are connected in series to generate high voltage (HV) with the overall efficiency higher than 80 %. Because the insulation requirement for each section is never more than the localized DC output of that section, the creepage distance of insulation in an ICT is smaller than in a conventional HV transformer. To further reduce the size, the planar ICT based on printed circuit boards (PCBs) at mid-frequency was proposed [6, 7].

However, the introduced insulation gaps result in magnetic flux leakage in an ICT, because the gaps ($\mu_r = 1$) have much higher reluctances compared to the magnetic core. This effect will cause a drop in magnetomotive force (MMF) and, accordingly, the output voltages from the secondary windings. The gap inductance is approximated by the reluctance model [7].

$$L = \frac{N^2}{R}, \quad R = \frac{l}{\mu_r \mu_0 A_s}, \quad (1)$$

where N is the number of turns of the primary winding, l is the dielectric thickness, μ_r is the relative permeability of the insulation material, and A_s is the effective cross-

This work was supported by National Natural Science Foundation of China (No. 11305068), and the “2011 project” organized by Hubei Collaboration Innovation Center of Non-power Nuclear Technology.

✉ Lei Cao
leicao@hust.edu.cn

¹ China Electric Power Research Institute, Nanjing 210003, China

² State Key Laboratory of Advanced Electromagnetic Engineering and Technology, Huazhong University of Science and Technology, Wuhan 430074, China

sectional area. Fringing flux at the gap periphery makes A_s larger than its physical area [8]. For the ICT with multiple insulation gaps, the equivalent gap inductance seen at each winding terminal will deviate from Eq. (1) and vary from one gap to another.

In addition, the leakage inductances between adjacent windings also reduce the magnetic flux more or less, depending on the locations and dimensions of the windings. Ideally, the leakage inductance between winding w_1 and w_2 can be estimated as follows [9].

$$L_{w_1w_2} = \frac{\mu_0 S N^2}{W^2} (H_a + H_{w_1}/3 + H_{w_2}/3), \tag{2}$$

where S is the winding cross-sectional area. W is the winding width. H_{w_1} and H_{w_2} are the height of winding w_1 and w_2 , respectively. H_a is the height of air region between w_1 and w_2 . Precise calculation of the winding leakage inductance requires knowing the magnetic field distribution [10]. Gaps between windings make the analytical calculation difficult in an ICT.

Transformer models are needed to accurately analyze and mitigate the above-mentioned leakage effect. Generally, the modeling methods can be classified into four groups. The first type is the finite element method (FEM). It is most accurate to simulate the transient response of three-dimensional (3D) transformers, but the method is time-consuming. It is used to validate the equivalent circuit model in this paper. The second group utilizes the impedance or admittance matrix, as in the electromagnetic transients program (EMTP) [11]. This black-box approach can be easily implanted, but the topology details of the transformers are missing. The third kind is based on the coupling between magnetic (transformer) and electrical (external circuit) equations taking into account core dimensions and material characteristics [12]. The 2D transformer model was developed, but a full 3D transformer structure has not been considered. The last group tries to establish the equivalent electrical circuit of transformers based on the principle of duality [13–15]. The model can be realized in commercial circuit software. The transformer model of the last group with multiple insulation layers (several millimeter thicknesses) in an ICT has not been reported in the literature.

This letter investigates for the first time the leakage phenomena for the design of a multi-winding ICT based on its physical nature. The leakage inductances between windings and the leakage inductances due to the insulation gaps are calculated numerically by winding a mutual inductances matrix. The unique feature of the leakage inductance model is to facilitate the analysis of the internal parameters and the steady-state response of an ICT. Section 2 gives a detailed process to construct the electrical circuit of a general multi-winding ICT based on the

principle of duality. In Sect. 3, the method to calculate each inductance in the equivalent circuit is demonstrated by converting the winding inductances matrix according to the terminal output characteristics. The typical example of a six-stage 2D ICT structure is analyzed by the proposed electrical circuit model in Sect. 4.

2 Equivalent circuit model

Figure 1 shows the ideal magnetic flux distribution in the multi-winding ICT with three core legs and top-bottom yokes. For the sake of simplicity, the rectifier circuits are not shown. Besides one primary winding (p) and n secondary windings ($s_1 \sim s_n$), there are n gaps ($g_1 \sim g_n$) located between adjacent cores in the central leg. The primary winding with larger cross section is at the bottom, while secondary windings are arranged accordingly at the upper sections. Due to the structural symmetry, one half of the geometry is used to illustrate the magnetic flux in the core and gaps ($\phi_{mp}, \phi_{m1} \sim \phi_{mn}$) and the leakage flux in the air (windings) region ($\phi_{s1} \sim \phi_{sn}$). The single-phase structure is sufficient to understand the leakage effects in an ICT. The leakage between windings on different core legs can be calculated using the same principle.

According to the flux paths in Fig. 1, the reluctance model is described in Fig. 2. R_m is the magnetizing reluctance. $R_{s1} \sim R_{sn}$ are the leakage reluctance between windings. $R_{g1} \sim R_{gn}$ are the reluctance associated principally with the gaps, and also with the surrounding magnetic cores. $N_p I_p, N_1 I_1 \sim N_n I_n$ are the assumed infinitely small

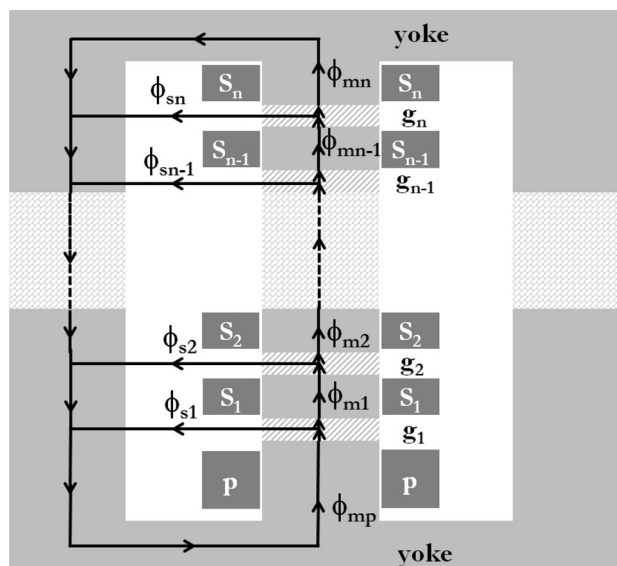


Fig. 1 Calculation model of an ICT with one leg having n secondary windings

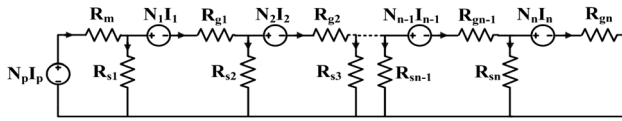


Fig. 2 Reluctance model of the ICT structure

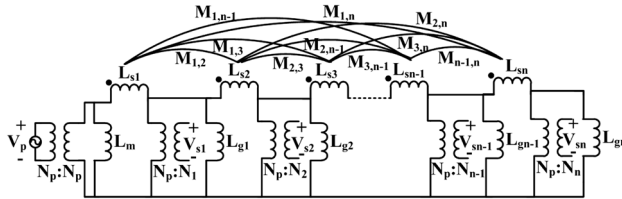


Fig. 3 Equivalent circuit model of the ICT structure

sources positioned at the center of the corresponding winding. Based on the principle of duality [15], the equivalent electrical circuit model is shown in Fig. 3 in the form of π network.

Both the magnetizing inductance, L_m (in parallel with the primary winding as in a traditional transformer), and the inductances $L_{g1} \sim L_{gn}$ (in parallel with the left side of the ideal transformer representing secondary windings) are influenced by the core properties, as well as gap dimensions. For the sake of simplicity, we call the special inductance $L_{g1} \sim L_{gn}$ in this letter to distinguish from the pure gap inductance in Eq. (1).

As discussed in Ref. [13], the winding leakage inductances, $L_{s1} \sim L_{sn}$, are mutually coupled with each other, due to the overlap of adjacent magnetic flux, Φ_{si} and Φ_{si+1} ($i = 1, 2, \dots, n - 1$). It was found in Ref. [16] that the equivalent π network of a multi-winding transformer without gaps is physically based, which can be mathematically converted into the form of a T network [17].

If there are no gaps, the circuit in Fig. 3 returns to the case in Ref. [14]. In order to design an ideal ICT without any flux leakage, $L_{s1} \sim L_{sn}$ should be as small as possible (ideally zero), while $L_{g1} \sim L_{gn}$ should be as large as possible (ideally infinite). In this situation, the secondary windings will have the same output voltage. The evaluation of the leakage phenomena in a real ICT depends on the calculation of leakage inductances, which relates critically to the magnetic field distribution in the interested computation regions.

However, the real flux pattern with both vertical and horizontal components will deviate from the assumed ideal case in Fig. 1, making the direct analytical calculation of the different reluctance or inductance components difficult via Eq. (1) and (2). The reluctance will have complicated

components connected in series or parallel form. The calculation of each component is not necessary because we only care about the equivalent reluctances/inductances seen at and between windings terminals. A numerical method is preferred to determine the leakage inductances in the next section.

3 Inductance determination

Generally, an inductance can be accurately calculated by the magnetic energy storage formula [9]

$$L = \frac{\mu_r \mu_0}{I^2} \iiint H^2 dv, \tag{3}$$

where H is the magnetic field intensity inside the volume of an inductor material with a relative permeability μ_r and I is the current flowing through the inductor.

Existing methods for characterizing the terminal output properties of a multi-winding transformer are usually based on the winding self- and mutual inductances matrix (M^w). Its elements are normally calculated through Eq. (3) in magnetostatic FEM simulations. For the ICT structure, its output voltages obtained by the equivalent circuit in Fig. 3 should be the same as the mathematical results predicted by M^w .

$$V_{(n+1) \times 1} = \omega M_{(n+1) \times (n+1)}^w I_{(n+1) \times 1}, \tag{4}$$

where $\omega = 2\pi f$ is the angular frequency. For the sake of computation convenience, the matrix is written in 2×2 block matrix form,

$$M_{(n+1) \times (n+1)}^w = \begin{pmatrix} M_{1 \times 1}^{(\omega 1)} & M_{1 \times n}^{(\omega 2)} \\ M_{n \times 1}^{(\omega 3)} & M_{n \times n}^{(\omega 4)} \end{pmatrix}. \tag{5}$$

By equating the voltage–current relationship at each winding terminal, the magnetizing inductance and gap-associated leakage inductances are expressed by

$$\begin{aligned} & (1/L_m, a_1/L_{g1}, \dots, a_n/L_{gn})_{1 \times (n+1)} \\ & = (1, -b_1, \dots, -b_n)_{1 \times (n+1)} (M_{(n+1) \times (n+1)}^w)^{-1}, \end{aligned} \tag{6}$$

where $a_n = N_p/N_n$ and $b_n = 1/a_n$.

The winding leakage inductance matrix is

$$M_{n \times n}^l = B(D + C(M_b)^{-1})^{-1}, \tag{7}$$

where

$$M_b = \omega(M^{(\omega 4)} - M^{(\omega 3)}M^{(\omega 2)}/M^{(\omega 1)}). \tag{8}$$

$$B_{n \times n} = \begin{pmatrix} -a_1 & 0 & 0 & \cdots & 0 \\ a_1 & -a_2 & 0 & \cdots & 0 \\ 0 & a_2 & -a_3 & \cdots & 0 \\ \vdots & \vdots & \vdots & \ddots & \vdots \\ 0 & \cdots & 0 & a_{n-1} & -a_n \end{pmatrix}, \tag{9}$$

$$C_{n \times n} = \omega \begin{pmatrix} b_1 & b_2 & b_3 & \cdots & b_n \\ 0 & b_2 & b_3 & \cdots & b_n \\ 0 & 0 & b_3 & \cdots & b_n \\ \vdots & \vdots & \vdots & \ddots & b_n \\ 0 & \cdots & 0 & 0 & b_n \end{pmatrix}, \tag{10}$$

$$D_{n \times n} = \begin{pmatrix} a_1/L_{g1} & a_2/L_{g2} & a_3/L_{g3} & \cdots & a_n/L_{gn} \\ 0 & a_2/L_{g2} & a_3/L_{g3} & \cdots & a_n/L_{gn} \\ 0 & 0 & a_3/L_{g3} & \cdots & a_n/L_{gn} \\ \vdots & \vdots & \vdots & \ddots & a_n/L_{gn} \\ 0 & \cdots & 0 & 0 & a_n/L_{gn} \end{pmatrix}. \tag{11}$$

The leakage inductances, $L_{s1} \sim L_{sn}$, are the diagonal elements of matrix $M'_{n \times n}$ and the mutual inductances, $M_{i,j}(i, j = 1, \dots, n, i \neq j)$, correspond to the non-diagonal elements. All the leakage inductances formulas have been derived based on the winding matrix M^w . In the next section, a six-stage ICT will serve to demonstrate the validity of the equivalent circuit model.

4 Example of a six-stage ICT

Figure 4 shows one half of the structure of the studied ICT with the indicated dimensions. It has six secondary windings with the same dimensions. The number of turns is 50 for the primary winding, and 1000 for all the secondary windings. The thickness of the insulation layer is 2 mm. A sinusoidal voltage source with a peak amplitude of 500 V and a frequency of 50 Hz is connected directly to the primary winding. Because of the linear inductances in the equivalent circuit, we assume that the magnetic core behaves linearly. The influences of core saturation on the leakage inductances will also be considered.

By manipulating the inductance matrix of the seven windings (p, s1 ~ s6), the calculated inductances per unit depth in the equivalent circuit are listed in Table 1 and Table 2. The winding leakage inductances (several mH) are much smaller than the magnetizing inductance and gap-associated leakage inductances (several tens of mH). The coupling between different winding leakage inductances is weak.

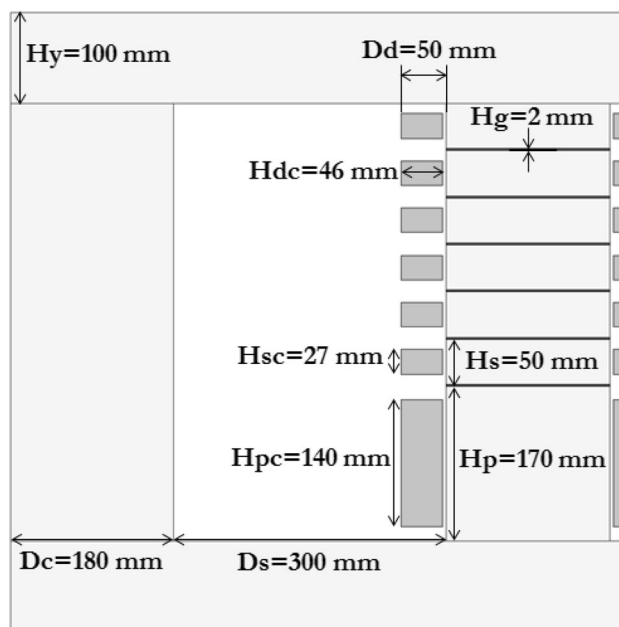


Fig. 4 Half geometry of a 2D ICT with six secondary windings

Table 1 Magnetizing inductance and gap-associated leakage inductances

L	Equivalent circuit (H)	Eq. (1) (H)	Core saturation (mH)	Without gap (H)
L_m	0.5914	–	2.3653	0.9540
L_{g1}	0.2190	0.2827	11.3844	5.6965
L_{g2}	0.2734	0.2827	10.6888	4.6990
L_{g3}	0.2699	0.2827	10.5646	4.5876
L_{g4}	0.2711	0.2827	10.2020	4.4150
L_{g5}	0.2558	0.2827	9.9503	4.2680
L_{g6}	0.5101	0.2827	4.6460	2.0620

The third column is the calculated gap inductances by Eq. (1) and winding leakage inductances by Eq. (2). Compared with the values of $L_{g1} \sim L_{g6}$ in Table 1, it is obvious that Eq. (1) cannot exactly predict the gap-associated leakage inductances seen at secondary winding terminals. The relative difference lies between 22 and 80 %. If the fringing field effect is considered, the pure gap inductance will increase by about 3 % [8]. This deviation mainly comes from the additional large core inductance not considered in Eq. (1). Indeed, if there are no gaps (insulation layers are replaced by magnetic cores), the calculated inductances $L_{g1} \sim L_{g6}$ are much higher, which is the solo contribution of magnetic cores, as shown in the last column of Table 1. It should be pointed out that the gap-associated inductances at secondary windings are different,

Table 2 Winding leakage inductance

L&M	Equivalent circuit (mH)	Eq. (2) (mH)	Core saturation (mH)	Without gap (mH)
L_{s1}	4.6429	4.2257	3.8291	4.6079
L_{s2}	3.1973	2.1589	2.9020	3.2028
L_{s3}	3.1975	2.1589	2.9082	3.2028
L_{s4}	3.2132	2.1589	2.9265	3.2029
L_{s5}	3.2649	2.1589	2.9760	3.2532
L_{s6}	3.5284	2.1589	3.0613	3.5286
$M_{s1,s2}$	0.6866	–	0.5073	0.6719
$M_{s1,s3}$	0.4491	–	0.2798	0.4481
$M_{s1,s4}$	0.2060	–	0.1309	0.1986
$M_{s1,s5}$	0.0988	–	0.0726	0.1239
$M_{s1,s6}$	0.0411	–	0.0404	0.0240
$M_{s2,s3}$	0.3987	–	0.3642	0.3984
$M_{s2,s4}$	0.3181	–	0.2148	0.3240
$M_{s2,s5}$	0.1339	–	0.0929	0.1243
$M_{s2,s6}$	0.0507	–	0.0464	0.0493
$M_{s3,s4}$	0.3938	–	0.3548	0.3984
$M_{s3,s5}$	0.3023	–	0.2079	0.2990
$M_{s3,s6}$	0.1080	–	0.0828	0.1242
$M_{s4,s5}$	0.3648	–	0.3401	0.3482
$M_{s4,s6}$	0.2514	–	0.1881	0.2488
$M_{s5,s6}$	0.2504	–	0.2882	0.2478

while most previous publications concerning ICT problems assume the same value [6, 7, 18].

On the other hand, analytic Eq. (2) underestimates the winding leakage inductance by 8.99 % (L_{s1}), 32.48 % (L_{s2} and L_{s3}), 32.81 % (L_{s4}), 33.87 % (L_{s5}), and 38.81 % (L_{s6}). The differences come from the assumptions in Eq. (2): The magnetic flux flows in the horizontal direction in the winding region; the magnetic field is trapezoidal along the direction of winding height; and the total amp-turns are zero between two adjacent windings. It is noted from the last column in Table 2 that the gaps have negligible influences on the winding leakage inductances. These results confirm the effectiveness of the equivalent circuit model, and specially, the mutual inductances between winding leakage inductances can also be determined.

In the worst case, when the magnetic core is highly saturated, the leakage inductances in the equivalent circuit are listed in the fourth column (note the different units in Table 1). The inductances $L_{g1} \sim L_{g6}$ are significantly reduced and become comparable with the winding leakage inductances in Table 2. Therefore, the magnetic flux in the ICT is seriously leaky. As a result, its output properties will deteriorate.

The peak amplitudes of the no-load output voltages from the six stages are listed in Table 3. The equivalent circuit is implanted in an electrical circuit simulator, and an

Table 3 Output voltages from six secondary windings

Stage	Equivalent circuit (kV)	FEM simu. (kV)	Core saturation (kV)	Without gap (kV)
V_{s1}	9.2887	9.2889	5.1574	9.9464
V_{s2}	9.0242	9.0243	3.3321	9.9218
V_{s3}	8.8487	8.8492	2.3012	9.9037
V_{s4}	8.7368	8.7367	1.6653	9.8895
V_{s5}	8.6790	8.6790	1.2511	9.8779
V_{s6}	8.6805	8.6802	0.9689	9.8676

independent transient FEM simulation is performed according to the ICT structure in Fig. 4. The results from the equivalent circuit method (second column) are verified by the FEM simulation (third column). The voltage difference between the first and sixth stage reaches 0.6082 kV. However, if the gaps are not present, the output voltages are uniform and the maximum difference is only 0.0788 kV in the last column of Table 3. As predicted, the voltages decrease and are highly inhomogeneous if the core saturates (fourth column). The excitation current passing through the primary winding increases up to 27 times the normal value. The large current will probably harm the ICT.

One method to eliminate the gap-associated flux leakage in an ICT is to add compensation capacitances at the output terminals of the secondary windings [6, 7, 18]. The values of capacitances are calculated by

$$C_n = a_n^2 / (\omega^2 L_{gn}), \tag{12}$$

where $a_n = 50/1000$. At the primary winding, the magnetizing inductance is usually compensated with a tuning capacitance ($C_m = 1/(\omega^2 L_m)$), as in a traditional transformer to reduce further the reactive power.

When the compensation capacitances C_n are positioned at the terminals of the secondary windings of the ICT, the output voltages become homogeneous and approach 10 kV, which is the secondary output of an ideal transformer with the turn ratio $N_p : N_s = 1 : 20$ ($V_p = 500$ V) without any leakage. These results are also confirmed by the traditional method with the winding inductance matrix. It should be stated that the circuit in Fig. 4 can also be used to study the steady-state response of a 3D ICT structure in case the secondary windings are loaded, short-circuited, and open-circuited.

5 Conclusion

In summary, a physically equivalent circuit was proposed to study the flux leakage effects in the insulated core transformer. The circuit can be implanted feasibly in

electrical circuit simulators. The circuit parameters were determined exactly by the traditional winding self- and mutual inductance matrix from magnetostatic FEM simulations. The major contribution of flux leakage is from the insulation gaps.

Although the equivalent circuit presented in this work is for ICT without losses (insulation layer, winding and core losses), it could be slightly modified to accommodate the loss nature of a 3D ICT.

References

- Z. Zimek, G. Przybytniak, A. Nowicki, Optimization of electron beam crosslinking of wire and cable insulation. *Radiat. Phys. Chem.* **81**, 1398–1403 (2012). doi:[10.1016/j.radphyschem.2012.01.028](https://doi.org/10.1016/j.radphyschem.2012.01.028)
- M.N. Martins, T.F. Silva, Electron accelerators: History, applications, and perspectives. *Radiat Phys Chem* **95**, 78–85 (2014). doi:[10.1016/j.radphyschem.2012.12.008](https://doi.org/10.1016/j.radphyschem.2012.12.008)
- P.G. Benny, S.A. Khader, K.S.S. Sarma, Dosimetric evaluation of multi-sided irradiation on HDPE pipes under 2 MeV electron beam. *Nucl. Instrum. Meth. A* **739**, 48–54 (2014). doi:[10.1016/j.nima.2013.12.023](https://doi.org/10.1016/j.nima.2013.12.023)
- M. Malo, A. Morono, E.R. Hodgson, Radioluminescence characterization of SiC and SiC/SiC for 1.8 MeV electron irradiation. *J. Nucl. Mater.* **442**, S404–S409 (2013). doi:[10.1016/j.jnucmat.2012.10.036](https://doi.org/10.1016/j.jnucmat.2012.10.036)
- R.J. Van de Graaff, US patent 3187208. High voltage electromagnetic apparatus having an insulating magnetic core **1**, (June 1965)
- U. Uhmeyer, KSI's cross insulated core transformer technology. The 18th International Spin Physics Symposium (SPIN2008), Charlottesville, USA. Oct. **6–11**, (2008)
- C. Kang, Y.H. Liu, D.M. Li, Analysis of output voltage on a planar insulating core transformer. *Nucl. Sci. Tech.* **22**, 15–18 (2011)
- A. Balakrishnan, W.T. Joines, T.G. Wilson, Air-gap reluctance and inductance calculations for magnetic circuits using a Schwarz-Christoffel transformation. *IEEE Trans. Power Electron.* **2**(4), 654–663 (1997). doi:[10.1109/63.602560](https://doi.org/10.1109/63.602560)
- M.D. Robert, P. Bertrand, T.F. Pierre, *Transformer Design Principles: With Applications to Core-Form Power Transformers* (CRC press, Florida, 2010), pp. 69–102
- D. Azizian, M. Vakilian, J. Faiz, A new multi-winding traction transformer equivalent circuit for short-circuit performance analysis. *Int. Trans. Electr. Energy Syst.* **24**(2), 186–202 (2014). doi:[10.1002/etep.1686](https://doi.org/10.1002/etep.1686)
- X. Chen, Negative inductance and numerical instability of the saturable transformer component in EMT. *IEEE Trans. Power Deliv.* **15**, 1199–1204 (2000). doi:[10.1109/61.891503](https://doi.org/10.1109/61.891503)
- A.D. Theocharis, J. Miliadis-Argitis, Th Zacharias, Single-phase transformer model including magnetic hysteresis and eddy currents. *Electr. Eng.* **90**, 229–241 (2008). doi:[10.1007/s00202-007-0071-5](https://doi.org/10.1007/s00202-007-0071-5)
- L. de Francisco, J.A. Martinez, Dual three-winding transformer equivalent circuit matching leakage measurements. *IEEE Trans. Power Deliv.* **24**, 160–168 (2009). doi:[10.1109/PES.2009.5275730](https://doi.org/10.1109/PES.2009.5275730)
- A.M. Casimiro, L. de Francisco, M.L.F. Xose, Equivalent circuit for the leakage inductance of multiwinding transformers: unification of terminal and duality models. *IEEE Trans. Power Deliv.* **27**(1), 353–361 (2012). doi:[10.1109/TPWRD.2011.2173216](https://doi.org/10.1109/TPWRD.2011.2173216)
- J. Saeed, L. de Francisco, Experimentally validated reversible single-phase multiwinding transformer model for the accurate calculation of low-frequency transients. *IEEE Trans. Power Deliv.* **30**, 193–201 (2015). doi:[10.1109/TPWRD.2014.2319093](https://doi.org/10.1109/TPWRD.2014.2319093)
- L. Mathieu, M.D. Manuel, M. Jean et al., Transformer leakage flux models for electromagnetic transients: critical review and validation of a new model. *IEEE Trans Power. Deliv.* **29**(5), 2180–2188 (2014). doi:[10.1109/TPWRD.2013.2293978](https://doi.org/10.1109/TPWRD.2013.2293978)
- W.L. Gerald, E.H. Sayed-Amr, Coupled inductance and reluctance models of magnetic components. *IEEE Trans. Power Electron.* **6**, 240–250 (1991). doi:[10.1109/63.76810](https://doi.org/10.1109/63.76810)
- L. Yang, J. Yang, K.F. Liu et al., A combined compensation method for the output voltage of an insulated core transformer power supply. *Rev. Sci. Instrum.* **85**, 063302 (2014). doi:[10.1063/1.4884340](https://doi.org/10.1063/1.4884340)